THERMAL CONDITIONS IN A LASER IN A LOW-DENSITY GAS

G. N. Dul'nev, V. A. Korablev,
A. E. Mikhailov, Yu. T. Nagibin,
V. G. Parfenov, and A. V. Sharkov

UDC 536.241:621.375.826

Thermal conditions are examined for a solid-state laser having natural cooling and working at atmospheric pressure or in a low-density gas. Measurements and calculations are reported on the nonstationary temperature distributions.

Simulation is applied to heat transfer in solid-state lasers with natural cooling as a basic stage in designing them [1]; it is particularly effective for lasers working under vacuum, because experiments are fairly difficult to perform.

It must be borne in mind that the results are affected by uncertainties in the input data (heat-transfer factor, surface blacknesses, and thermal resistances) if one is to interpret the results correctly and to define the permissible errors in the model. Here we examine those effects for a two-lamp laser as shown in Fig. 1, which works either in air at normal pressure or in a low-density gas. Within the body 1, whose inner surface has a diffusely reflecting coating, there is the rod 2 consisting of yttrium aluminum garnet activated with neodymium, diameter 8 mm and length 80 mm, and two pumping lamps 3, type INP 3/75. The rod is placed in a transparent conducting white sapphire tube 4 with a gap of about 0.1-0.2 mm, which is linked by the indium inserts 5 to the body. The components form a close-packed pumping system. The laser works with a pulse repetition frequency of 0.2 Hz at a pumping energy of 60 J for 1000 sec.

We also examined the performance from various measures to improve the laser cooling, particularly for two basic modes of cooling: without a special conductive arrangement on the outer surface and with a metal chassis; we also examined the effect from an immersion medium between the sapphite and the rod. The simulation results were compared with measurements. The heat source distributions were calculated from a Monte Carlo suite [2]. The thermophysical processes were simulated by means of a suite employing the numerical method described in [3]. The temperature patterns were determined by solving the nonstationary multidimensional conduction equations.

The apparatus included a Mach—Zender interferometer, whose essentials are shown in Fig. 2. The beam from the helium—neon laser 1 (LG-38) was expanded by the telescope system 2 and 3 and reached the beam-splitting cube 4. Spatial filtration was provided by the stop 5. The object beam passed through the beam splitter 4 and rod 6 and was reflected from the mirror 7 in the beam splitter cube 8 and reached the lens 9. The reference beam was reflected from the beam splitter 4 and mirror 10 and passed through beam splitter 8 and also reached the lens 9. The two intensities were equalized to produce the maximum contrast in

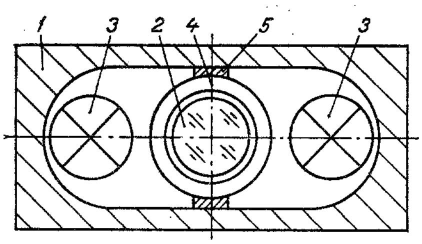

Fig. 1. The laser.

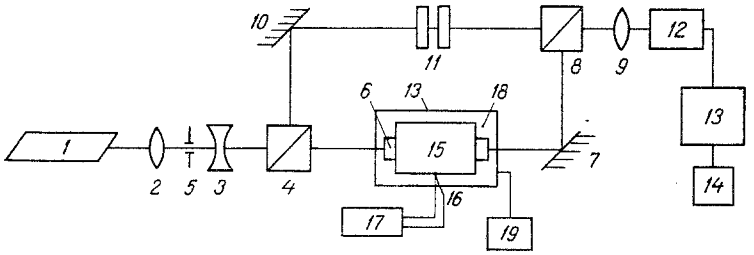

Fig. 2. The apparatus.

Leningrad Fine Mechanics and Optics Institute. Translated from Inzhenerno-Fizicheskii Zhurnal, Vol. 55, No. 5, pp. 842-847, November, 1988. Original article submitted July 2, 1987.

the interference pattern, which was provided by the neutral filters 11. Lens 9 imaged the rod in the plane of the TV camera 12. The interferometer was adjusted to give finite-width fringes. The changes in the pattern on rod heating were recorded by the video tape recorder 13 and displayed on the monitor 14. The rod temperature was determined from the number of fringes passing through the center of the image. The temperature at the outer surface of the body 15 was measured by the chromel-copel thermocouple 16 and digital voltmeter 17 (V7-23). The laser was set up in the vacuum chamber 18, where the pressure was monitored by the gauge 19 (VIT-2).

We consider the heat-transfer mechanisms in the laser and the models used in the thermal calculations. The heat transfer in air is by conduction and radiation; there is no convection in the reflector cavity because the gaps δ between the components are so small that the Rayleigh condition $Ra_\delta < 1000$ [4]. We simulated the conduction in the narrow annular gap between the rod and tube by taking the heat-flux vector as perpendicular to the surfaces, while transport along the channels was neglected. Conduction in the reflector cavity was described by the multidimensional equation for an immobile gas. The radiative transfer was calculated with the surface taken as gray, diffusely reflecting, and radiating. The radiative transfer in the reflector cavity was described in the three-dimensional approximation [5]. When the chassis was incorporated, the coupling to the body was described in terms of a contact resistance, which was determined by the methods of [6]. When there was none, the heat was removed from the surface of the body by radiation and free convection. The heat-transfer coefficients for the outer surface in free convection were determined from standard dimensionless formulas [7].

Radiation makes the main contribution to the heat transfer at the outer surface of the body and between the components in vacuum. Even at 10 Pa, one can neglect the contribution from conduction to the total transfer. Calculations from [8] show that the thermal conductivity in a low-density gas in the reflector cavity and in the gap between the rod and tube is less by about a factor 30 than that for air at atmospheric pressure. At higher pressures, one needs to incorporate the conduction, particularly the pressure dependence.

The rod temperature rises substantially in the low-density gas because of reduced coupling to the tube due to the lack of conduction between them. One can accelerate the transfer in the gap with an immersion medium. We examined that model. The conductivity transfer in the gap was incorporated in the above approximation.

We examined how uncertainties in the input affected the simulation calculations (heat-transfer coefficients, contact resistances, and surface blackness), where we used statistical methods with the algorithm of [9]. We performed a series of calculations with input data randomly selected from set ranges, in which the distributions were taken as uniform, and from which we constructed interval estimators for the mean rod temperature.

Figures 3 and 4 show the corridors for the mean temperature rises in the rod and body due to uncertainty in the input parameters: blacknesses in the rod, tube, pumping lamps, reflective coating, and body (uncertainty range 0.7-1), the contact resistance between the body and the conductive cooler (0.1-0.5 K/W), the thermal resistance represented by the in-

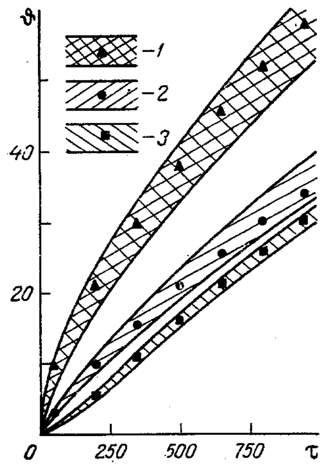

Fig. 3. Mean temperature rise ϑ in K in laser elements as functions of time τ in sec without immersion: 1 and 2) rods at 10 Pa and 10^5 Pa; 3) body.

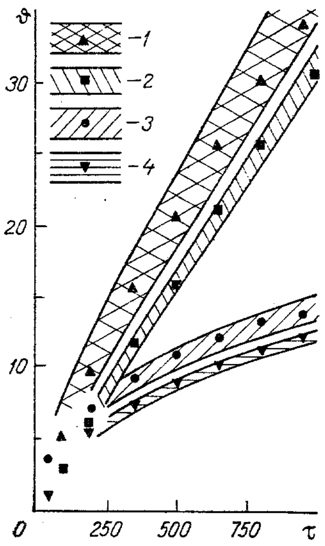

Fig. 4. Mean temperature rises ϑ for laser elements as functions of time τ with immersion at 10 Pa: 1) rod; 2) body; 3) rod with special conductive cooling; 4) body with special conductive cooling.

dium inserts arising from fluctuations in thickness and tube contact area (0.1-0.3 K/W), heat-transfer coefficient for the body (4-6 $W/m^2 \cdot K$), and resistance in the gap filled with immersion medium (0.1-0.3 K/W). The various parameters affected the results in different ways. For example, the range in rod temperature rise associated with uncertainty in the blacknesses was 4% (relative to the middle of the range), while that from the contact resistance in the indium was 4%, that from the heat-transfer coefficient for the body 16%, and that from the gap resistance 5-8%.

These models were tested for adequacy by comparing the calculated mean temperature rises with measurements on various styles of laser working at normal pressure and at 10 Pa.

The calculations showed that the rod temperature pattern was almost uniform throughout the operation. The maximum temperature difference over the cross section (at the end of the pumping pulse) was 1-1.2 K, while in the intervals between pulses, the temperatures equalized completely because the garnet is of high thermal conductivity, which was confirmed by measurement.

Figures 3 and 4 show the measurements and calculations on the rod heating. The hatched regions correspond to the calculated spreads due to input uncertainty, while the points are measurements. Test results without immersion in air and in vacuum showed that the rod temperature was much higher in the latter case (curves 1 and 2 in Fig. 3). The reduced thermal resistance from the immersion lowers the rod heating in vacuum by a factor 2-3 (curves 1 in Figs. 3 and 4), where the temperature differences between the rod and body was 4-6 K (curves 2 and 3 in Fig. 3).

When the laser works in air, the immersion has hardly any effect on the temperature. The rises in temperature in rod and body were almost the same with and without immersion, because the conductivity in the air gap between rod and tube was quite high with or without immersion as the gap was only 0.1-0.2 mm. The main contribution to the total resistance between rod and environment comes from the contact between the body and the environment, as this is governed by the fairly low heat-transfer coefficient at the body.

One can reduce the body and rod temperatures by providing good contact between the body and a special conductive cooler (metal chassis) having high heat capacity. Those conditions were simulated by inserting K-300 cement in narrow gaps between the body and chassis. Curves 3 and 4 in Fig. 4 show measurements and calculations on the rod and body with immersion and such body contact. The body temperature rise at the end of the cycle was less by a factor 1.8-2 than without the contact, and the rod temperature was correspondingly reduced.

The calculations and measurements thus show that these models represent the actual physical pattern adequately.

Input uncertainties cause differences in the simulation results of about 10-20%, so there is no need to reduce the errors in the numerical calculations below a few percent.

Immersion in a solid-state laser with natural cooling under vacuum reduces the rod temperature rise substantially. A similar effect is provided by conductive heat transfer at the surface.

LITERATURE CITED

1. G. N. Dul'nev, V. V. Barantsev, A. E. Mikhailov, et al., Zh. Tekh. Fiz., 57, No. 1, 98-102 (1987).
2. L. A. Savintseva, A. V. Sharkov, V. G. Parfenov, and V. A. Gur'yanov, Izv. Vyssh. Uchebn. Zaved., Priborostr., 23, No. 8, 92-96 (1981).
3. G. N. Dul'ev, A. E. Mikhailov, and V. G. Parfenov, Inzh.-Fiz. Zh., 53, No. 1, 107-113 (1987).
4. V. P. Isachenko, V. A. Osipova, and A. S. Sukomel, Heat Transfer [in Russian], Moscow (1981).
5. R. Siegel and J. Howell, Radiative Heat Transfer [Russian translation], Moscow (1975).
6. G. N. Dul'nev, Heat and Mass Transfer in Electronic Equipment [in Russian], Moscow (1984).
7. O. G. Martynenko and Yu. A. Sokovishin, Heat Transfer by Free Convection [in Russian], Minsk (1982).
8. M. Devien, Low-Density Gas Flow and Heat Transfer [Russian translation], Moscow (1962).
9. I. A. Glebov, G. N. Dul'nev, A. Yu. Potyagailo, and A. V. Sigalov, Izv. Akad. Nauk SSSR, Energ. Transport, No. 2, 70-77 (1982).